

# $\eta$ - $\eta'$ mixing determination from semileptonic $D_{(s)}^+$ and $B^+$ meson decays

Author: Joel Rastrojo Morote, jrastrmo7@alumnes.ub.edu  
Facultat de Física, Universitat de Barcelona, Diagonal 645, 08028 Barcelona, Spain.

Advisor: Sergi González-Solís de la Fuente, sergig@fqa.ub.edu

**Abstract:** In this work, we determine the degree of mixing of the  $\eta$  and  $\eta'$  mesons from the exclusive semileptonic  $D_{(s)}^+ \rightarrow \eta^{(\prime)} \ell^+ \nu_\ell$  and  $B^+ \rightarrow \eta^{(\prime)} \ell^+ \nu_\ell$  decays. A controlled parametrization of the participating hadronic form factor,  $D_{(s)} \rightarrow \eta^{(\prime)}$  and  $B \rightarrow \eta^{(\prime)}$ , in combination with experimental measurements, has allowed us to determine  $\phi = 40.6(4.8)^\circ$  and  $\phi = 42.3(3.7)^\circ$  from the analyses of differential decay width distributions and ratios of branching ratios, respectively. Our results are in good agreement with a recent determination from the Lattice QCD Extended Twisted Mass Collaboration,  $\phi = 39.3(2.0)^\circ$ , and larger than the naive estimate we calculate from Chiral Perturbation Theory at leading order  $\phi = 33.5^\circ$ .

**Keywords:**  $\eta$ - $\eta'$  physics, hadronic form factors, semileptonic meson decays

**SDGs:** 4. Quality education.

## I. INTRODUCTION

The  $\eta$  and  $\eta'$  are the lightest pseudoscalar mesons alongside the pions and kaons. Their masses are primarily generated by the spontaneous breaking of chiral symmetry in QCD. However, the  $\eta$  and  $\eta'$  have significantly higher masses than the pions, and their properties are strongly influenced by the  $U(1)$  axial anomaly. Unlike the other pseudoscalar mesons, the  $\eta$  and  $\eta'$  acquire a substantial portion of their mass from the  $U(1)$  anomaly. This anomaly breaks the classical  $U(1)$  symmetry of the QCD Lagrangian at the quantum level, leading to a mixing between the singlet and octet states. This mixing is crucial for understanding their observed masses. Accurate knowledge of  $\eta$  and  $\eta'$  properties, including their mixing parameters, is crucial for various phenomenological applications. They play a role in understanding low-energy hadron physics, probing the QCD vacuum, and are relevant for studying certain rare decays.

The mixing scheme have been analyzed in the context of Chiral Perturbation Theory -the low-energy Effective Field Theory of QCD for light mesons- and also recently by Lattice QCD collaborations. The degree of mixing is accounted by the so-called mixing angle  $\phi$  (in the quark-flavor basis), and just for orientation, the degree of mixing is about  $\phi = 35^\circ$  [1]. In this work, we will perform a phenomenological analysis of semileptonic  $D$  and  $B$  meson decays to determine the  $\eta$  and  $\eta'$  mixing. In particular, we will analyze the  $D_{(s)}^+ \rightarrow \eta^{(\prime)} \ell^+ \nu_\ell$  and  $B^+ \rightarrow \eta^{(\prime)} \ell^+ \nu_\ell$  decays experimental data to extract this mixing. The structure of this paper is as follows. The theoretical framework is given in Sec. II, where the participant form factors are defined. In Sec. III we perform our fits to extract the mixing from experimental data. In Sec. IV we briefly introduce the Chiral Lagrangian at leading order and provide and estimate of this mixing. Finally, in Section V, we present our conclusions.

## II. THEORETICAL FRAMEWORK

### A. SU(3) flavor pseudoscalar multiplet description

Mesons are hadrons formed by couples quark-antiquark, and can be classified in terms of their total angular momentum  $J$ , parity  $P$  and charge conjugation  $C$ . In our case, we will study pseudoscalar mesons, which are those with  $J^{PC} = 0^{-+}$ , concretely the multiplet conformed by  $u$ ,  $d$  and  $s$  flavors. Since  $m_u \approx m_d$  and both quarks experience the same intensity for strong interaction, a new flavor symmetry SU(2) is defined: the isospin, with its own generators. This allows us to classify the mesons forming a triplet of isospin  $I = 1$  with  $I_3 = -1, 0, 1$  and a singlet of  $I = 0$  with  $I_3 = 0$ . We use a rougher approximation that expands the symmetry to include  $s$  quarks but does not take into account the fact that  $m_s$  is larger than  $m_{u(d)}$ , in order to organize the mesons in multiplets, resulting in the SU(3) symmetry. We follow up by defining a new quantum number: the hypercharge  $Y$ , in order to keep characterizing the different resulting mesons. Since we have a 3 quark space and a 3 antiquarks' space, we obtain  $3 \otimes \bar{3} = 8 \oplus 1$ . Therefore, we will have an octet connected through the symmetry generator operators and a singlet that cannot be connected. In terms of the quantum numbers previously discussed, pions have  $I = 1$ ,  $Y = 0$  and are distinguished by  $I_3$ , meanwhile kaons have  $I = 1/2$  and are distinguished by  $I_3$  and  $Y$ , and finally for  $\eta_8$  and  $\eta_0$  these quantum numbers are all equal to 0. Thereafter, we will focus on  $\pi^0$ ,  $\eta_8$  and the singlet state  $\eta_0$ . Their quark content is:

$$\pi^0 = \frac{1}{\sqrt{2}} (u\bar{u} - d\bar{d}), \quad \eta_8 = \frac{1}{\sqrt{6}} (u\bar{u} + d\bar{d} - 2s\bar{s}), \quad \eta_0 = \frac{1}{\sqrt{3}} (u\bar{u} + d\bar{d} + s\bar{s}). \quad (1)$$

In Fig. 1, we present the structure of the pseudoscalar nonet:

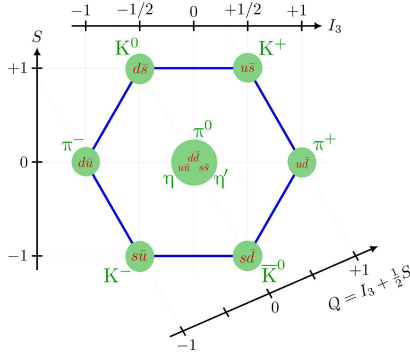


FIG. 1: Sketch of the SU(3) pseudoscalar nonet.

Due to the fact that SU(3) is not a perfect symmetry,  $\eta_8$  and  $\eta_0$  mix to form the physical  $\eta$  and  $\eta'$  mesons. This mixing can be parametrized, in the so-called octet-singlet basis, as:

$$\begin{pmatrix} \eta \\ \eta' \end{pmatrix} = \begin{pmatrix} \cos \theta & -\sin \theta \\ \sin \theta & \cos \theta \end{pmatrix} \begin{pmatrix} \eta_8 \\ \eta_0 \end{pmatrix}, \quad (2)$$

where the angle  $\theta$  accounts for the degree of admixture.

Another popular basis is the so-called quark-flavor, with  $\eta_q = \frac{1}{\sqrt{2}}(u\bar{u} + d\bar{d})$  and  $\eta_s = s\bar{s}$ , that separates the light quark content from the  $s\bar{s}$  content, and is given by the rotation:

$$\begin{pmatrix} \eta \\ \eta' \end{pmatrix} = \begin{pmatrix} \cos \phi & -\sin \phi \\ \sin \phi & \cos \phi \end{pmatrix} \begin{pmatrix} \eta_q \\ \eta_s \end{pmatrix}, \quad (3)$$

where the mixing angle  $\phi$  is related to the one obtained from Eq. (2) through:

$$\theta = \phi - \arctan \sqrt{2} \simeq \phi - 54.7^\circ. \quad (4)$$

This basis is specially useful given that it will allow us to study each decay from the point of view of light quark content against strange quark content. This will moreover enable us to parametrize the  $D^+$  and  $B^+$  decays with analogous expressions, due to the SU(2) symmetry between light quarks.

### B. Differential distributions for decays

Decays are the spontaneous breaking of one particle onto two or more particles which must be less massive. In our case, we will be working with decays led by weak and strong interactions, since the decays we will study are  $M_i \rightarrow M_f \ell^+ \nu_\ell$ , where  $M_i$  and  $M_f$  are the initial and final mesons that only involve the change in flavor of one quark. The physics of a such decay are described by the next equation, which can be derived from Fermi's golden rule, and considering our leptons are  $\mu^+$ ,  $e^+$  and neutrinos that are medium-light massed:

$$\frac{d\Gamma(M_i \rightarrow M_f \ell^+ \nu_\ell)}{dq^2} = \frac{G_F^2 |V_{q_i q_f}|^2}{24\pi^3} |\vec{P}_{M_f}(q^2)|^3 \times \left(1 - \frac{m_{\ell^+}^2}{q^2}\right)^2 \left(1 + \frac{m_{\ell^+}^2}{2q^2}\right) |f_+^{M_i \rightarrow M_f}(q^2)|^2, \quad (5)$$

where  $\vec{P}_{M_f}(q^2)$  is the momentum of the final particle in the initial particle rest frame divided by  $2m_{M_i}$ :

$$|\vec{P}_{M_f}(q^2)| = \frac{1}{2m_{M_i}} \sqrt{(m_{M_i}^2 + m_{M_f}^2 - q^2)^2 - 4m_{M_i}^2 m_{M_f}^2}, \quad (6)$$

$G_F$  is the Fermi constant and  $|V_{q_i q_f}|$  is the corresponding component of the Cabibbo-Kobayashi-Maskawa matrix, which governs the strength of the  $q_i \rightarrow q_f$  transition. For our analysis, we take all numerical input from the PDG [1].  $\Gamma$  is the partial decay width and somewhat measures the probability that the meson will decay through this channel. Finally,  $q^2$  is the invariant mass of the lepton pair in the final state and  $f_+^{M_i \rightarrow M_f}(q^2)$  is the form factor encoding the hadronic information, which will be explained in the following section.

### C. Form factors

Form factors are the functions that portray the internal structure of particles, in our case mesons. This avoids considering our mesons as punctual non-structured particles, giving them an internal gross distribution of their properties. In our study, we will consider two different parametrizations for the form factor: a monopole and a dipole structure. In Fig. 2 we introduce the quark diagrams for the decays:

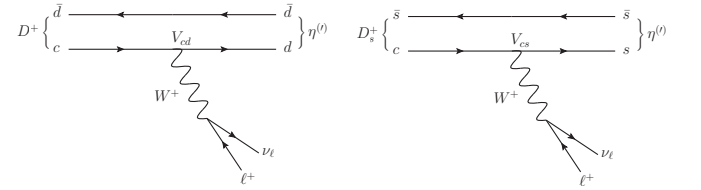


FIG. 2:  $D_{(s)}^+ \rightarrow \eta^{(\prime)} \ell^+ \nu_\ell$  decays at the quark level.

We observe that these decays occur through a  $W^+$  boson, producing a lepton-neutrino couple. In  $D^+$  decay there is an exchange of a  $c$  to a  $d$  quark, that is analogous to the  $\bar{b}$  to  $\bar{u}$  antiquark exchange in  $B^+$  decay. As we had seen in Sec. II A, all parametrization will be equal except for the value of the constants, since in both decays we are testing light quarks content.

If we focus only on the hadronic terms for the decay  $D(B)^+ \rightarrow \eta^{(\prime)}$ , we can use Eq. (3) and so we can approximate the form factors of  $D^+ \rightarrow \eta_{d\bar{d}(u\bar{u})}$  to those of  $D(B)^+ \rightarrow \pi^0$ , given that they have the same light quark components. This results in:

$$\begin{aligned} f_+^{D(B)^+ \rightarrow \eta}(q^2) &= \cos \phi f_+^{D(B)^+ \rightarrow \eta_{d\bar{d}(u\bar{u})}}(q^2) \\ &\simeq \cos \phi f_+^{D(B)^+ \rightarrow \pi^0}(q^2), \\ f_+^{D(B)^+ \rightarrow \eta'}(q^2) &= \sin \phi f_+^{D(B)^+ \rightarrow \eta_{d\bar{d}(u\bar{u})}}(q^2) \\ &\simeq \sin \phi f_+^{D(B)^+ \rightarrow \pi^0}(q^2), \end{aligned} \quad (7)$$

where we will parametrize  $f_+^{D(B)^+ \rightarrow \pi^0}(q^2)$  with the next monopole and dipole expressions:

$$f_+^{D(B)^+ \rightarrow \pi^0}(q^2) = \frac{f_+^{D(B)^+ \rightarrow \pi^0}(0)}{1 - \frac{q^2}{m_{D(B)^*}^2}},$$

$$f_+^{D(B)^+ \rightarrow \eta}(q^2) = \frac{f_+^{D(B)^+ \rightarrow \pi^0}(0)}{\left(1 - \frac{q^2}{m_{D(B)^*}^2}\right) \left(1 - \alpha \frac{q^2}{m_{D(B)^*}^2}\right)}, \quad (8)$$

where  $f_+^{D(B)^+ \rightarrow \pi^0}(0)$  is the form factor at zero momentum transfer, *e.g.*,  $f_+^{D^+ \rightarrow \pi^0}(0) = 0.6300$  from the Fermi-Lab Lattice QCD Collaboration [2],  $m_{D(B)^*}$  is the mass of the excited resonance and where  $\alpha$  is a free parameter that will be fitted and will allow us to write a second pole with an effective excited state mass.

In an analogous way to  $D_s$  decays, in Fig. 2 we notice that there is an exchange from a  $c$  to an  $s$  quark. In this case, when the rotation is applied to flavor base Eq. (3), we obtain:

$$f_+^{D_s^+ \rightarrow \eta}(q^2) = -\sin \phi f_+^{D_s^+ \rightarrow \eta s \bar{s}}(q^2),$$

$$f_+^{D_s^+ \rightarrow \eta'}(q^2) = \cos \phi f_+^{D_s^+ \rightarrow \eta s \bar{s}}(q^2). \quad (9)$$

As before, we describe  $f_+^{D_s^+ \rightarrow \eta s \bar{s}}(q^2)$  with a monopole and dipole form factors. For the monopole we write:

$$f_+^{D_s^+ \rightarrow \eta}(q^2) = -\sin \phi \frac{f_+^{D_s^+ \rightarrow \eta s \bar{s}}(0)}{1 - \frac{q^2}{m_{D_s^*}^2}},$$

$$f_+^{D_s^+ \rightarrow \eta'}(q^2) = \cos \phi \frac{f_+^{D_s^+ \rightarrow \eta s \bar{s}}(0)}{1 - \frac{q^2}{m_{D_s^*}^2}}, \quad (10)$$

while the expression for the dipole proceeds in an analogous fashion as in the previous case.

### III. MIXING ANGLE DETERMINATION

Once the elements needed to obtain an experimental value for the mixing angle are introduced, we will compute it following two different paths. The first technique uses the values given by the literature of differential distribution for decays Eq. (5) in small finite ranges, and the form factors discussed in Sec. II C. The second technique consists of computing the quotient of the numerical integral of differential decay width Eq. (5) with monopoles form factors, for the complete range of  $q^2$  from different decay channels for the same particle, which is equal to the quotient of branching ratios as will be presented in Sec. III B. This method of computing makes constants cancel themselves, allowing us to obtain a numerical value for the mixing angle.

### A. Fits to decay distributions

In the next sections we will be fitting Eq. (5) with the corresponding form factors and sets of data to obtain values for the mixing angle.

We start analyzing the  $D^+ \rightarrow \eta^{(\prime)} \ell^+ \nu_\ell$  decays. The data for the fits is from [3] and they are two sets of values for  $D^+ \rightarrow \eta \ell^+ \nu_\ell$ , that originate from different subchannels,  $D^+ \rightarrow \eta \gamma \gamma (\pi^0 \pi^+ \pi^-) \ell^+ \nu_\ell$ . We will not study these two subchannels separately, since both involve the same first decay to  $\eta$ , which is the one we are studying. For  $D^+ \rightarrow \eta' \ell^+ \nu_\ell$  we obtain the values from [4]. These data were obtained from experiments of BESIII collaboration, considering that those of  $\eta$  are notably recent. The form factors utilised are Eq. (8) combined with Eq. (7). Graphics from Fig. 3 represent the differential decay width fitted to monopoles and dipoles for  $D^+ \rightarrow \eta^{(\prime)} \ell^+ \nu_\ell$ . Results of each fit are shown in Table I.

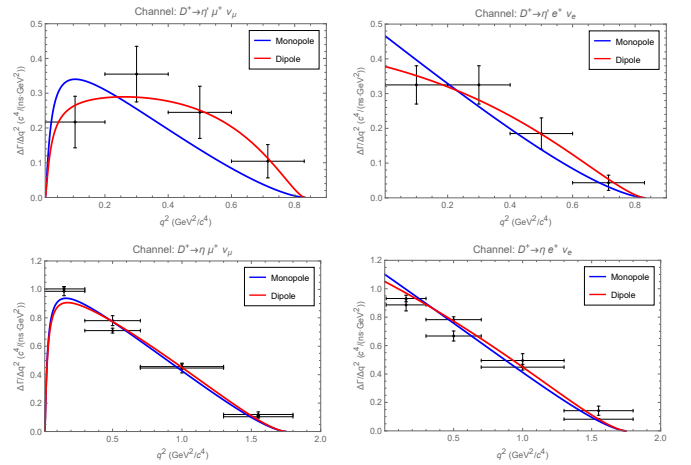


FIG. 3: Representation of the differential decay width for  $D^+ \rightarrow \eta^{(\prime)} \ell^+ \nu_\ell$  different channels with their corresponding fits to monopole and dipole model.

We next analyze the  $D_s^+ \rightarrow \eta^{(\prime)} e^+ \nu_e$  decays. All the data for the fits are obtained from [5], acquired from an experiment of BESIII collaboration. In this case, we have two sets of values for each channel since data came from two different subchannels:  $D_s^+ \rightarrow \eta \gamma \gamma (\pi^0 \pi^+ \pi^-) e^+ \nu_e$  and  $D_s^+ \rightarrow \eta' \eta \gamma \gamma \pi^+ \pi^- (\gamma \rho^0) e^+ \nu_e$ . Again, we will not study them separately given that the first decays of both subchannels are the ones we are studying. The form factors used for this decays are shown in Eq. (10), where  $f_+^{D_s^+ \rightarrow \eta'}$ ,  $\phi$  and  $\alpha$  must be fitted. The difficulty stems from the product of  $f_+^{D_s^+ \rightarrow \eta'}$  and  $\sin(\phi)$  or  $\cos(\phi)$ , that can be fitted but not for each component individually. To solve this issue we perform a combined fit to all sets of data with their corresponding form factors, due to the fact that they have the same parameters but different functions. In Fig. 4 we represent the differential decay width fitted to monopoles and dipoles for  $D_s^+ \rightarrow \eta^{(\prime)} e^+ \nu_e$  while in Table I we collect our fit results. As seen, all our deter-

minations are compatible within errors and the quality of the fits is good according to the  $\chi^2/dof$ .

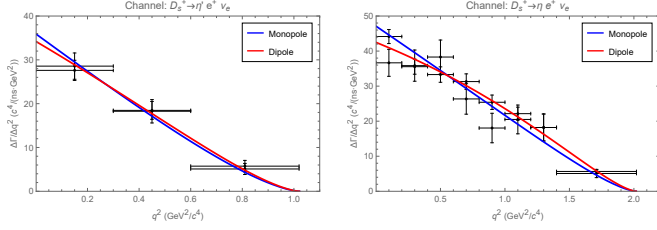


FIG. 4: Representation of the differential decay width for  $D_s^+ \rightarrow \eta^{(\prime)} e^+ \nu_e$  different channels with their corresponding combined fits to monopole and dipole model.

TABLE I: Values and errors of the different parameters fitted for each model for the different decay channels with their corresponding  $\chi^2_{dof}$  divided by the number of degrees of freedom.

Decay channel	Monopole		Dipole		
	$\phi$ ( $^\circ$ )	$\chi^2_{dof}$	$\phi$ ( $^\circ$ )	$\alpha$	$\chi^2_{dof}$
$D^+ \rightarrow \eta' \mu^+ \nu_\mu$	40.0(4.1)	2.89	31.3(4.2)	3.2(6)	0.57
$D^+ \rightarrow \eta' e^+ \nu_e$	39.3(2.5)	1.45	34.8(3.3)	1.8(8)	0.54
$D^+ \rightarrow \eta \mu^+ \nu_\mu$	43.5(4)	3.46	45.0(6)	0.21(6)	2.55
$D^+ \rightarrow \eta e^+ \nu_e$	45.1(3)	5.48	46.4(5)	0.26(7)	4.59
$D_s^+ \rightarrow \eta^{(\prime)} e^+ \nu_e$	40.8(8)	1.57	40.0(8)	0.4(1)	0.72

### B. Extraction from ratio of branching ratios

The branching ratio for one channel is defined as the probability to decay on this channel related to the probability of all possible modes. Its expression is  $BR(i) = \frac{\Gamma(i)}{\Gamma_{total}}$ , where  $i$  indicates the decay channel. We will compute  $\Gamma(i)$  integrating Eq. (5) for the complete range of values of  $q^2$ . If we compute the ratios from two different channels, for example  $R_{\eta'/\eta} \equiv \frac{BR(D_s^+ \rightarrow \eta' e^+ \nu_e)}{BR(D_s^+ \rightarrow \eta e^+ \nu_e)} = 0.35(2)$ , and we equate it to the quotient of integrals of Eq. (5) that can be performed numerically we obtain:

$$R_{\eta'/\eta} = |\tan \phi|^2 \frac{\int_{m_e^2}^{(m_{D_s^+} - m_{\eta'})^2} |\vec{P}_{\eta'}(q^2)|^3}{\int_{m_e^2}^{(m_{D_s^+} - m_\eta)^2} |\vec{P}_\eta(q^2)|^3} \times \frac{\left(1 - \frac{m_{e^+}^2}{q^2}\right)^2 \left(1 + \frac{m_{e^+}^2}{2q^2}\right) |f_+^{D_s^+ \rightarrow \eta'}(q^2)|^2 dq^2}{\left(1 - \frac{m_{e^+}^2}{q^2}\right)^2 \left(1 + \frac{m_{e^+}^2}{2q^2}\right) |f_+^{D_s^+ \rightarrow \eta}(q^2)|^2 dq^2}, \quad (11)$$

where we use the monopoles' expressions from Eqs. (8) and (10) as form factors, completing it with Eq. (7). From this expression we can obtain  $\phi$ ,

$$\phi = 41.1(8)^\circ. \quad (12)$$

This calculus can be done for all the combinations of the different channels, using the values from Table II of the

appendix. Individual results of all possible computations of  $\phi$  are presented in Table III of the appendix.

### C. Results

By conducting fits to the distributions for decays, we achieved the results from Table I, with an average and error of

$$\phi = 40.6(4.8)^\circ. \quad (13)$$

Moreover, from calculations using branching ratios, we obtained the values in Table III, with an average and error of

$$\phi = 42.3(3.7)^\circ, \quad (14)$$

where the errors correspond to their respective standard deviations, since the uncertainties obtained through error propagation are minimal and no longer reliable. All these values are shown in Fig. 5. Note that these values are in agreement with the very recent extraction by the ETM Lattice QCD Collaboration,  $\phi = 39.3(2.0)^\circ$  [6].

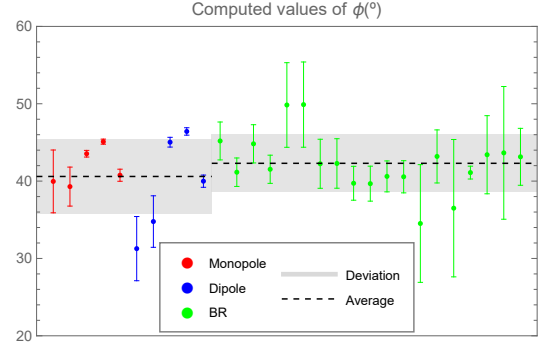


FIG. 5: Summary of our  $\eta$ - $\eta'$  mixing angle determinations.

### IV. THEORETICAL ESTIMATE OF THE MIXING ANGLE FROM CHPT

First, we have the Chiral Perturbation Theory Leading Order Lagrangian [7]:

$$\begin{aligned} \mathcal{L}^{\chi PT @ LO} &= \frac{f_\pi^2}{4} \text{Tr} [\partial_\mu U^\dagger \partial^\mu U] \\ &+ \frac{f_\pi^2}{4} \text{Tr} [2B_0(\mathcal{M}U + \mathcal{M}U^\dagger)] - \frac{1}{2} m_0^2 \eta^2, \\ \mathcal{M} &= \begin{pmatrix} m_u & 0 & 0 \\ 0 & m_d & 0 \\ 0 & 0 & m_s \end{pmatrix}, \quad U = \exp\left(\frac{i\sqrt{2}\Phi}{f_\pi}\right), \\ \Phi &= \begin{pmatrix} \frac{1}{\sqrt{2}}\pi^0 + \frac{1}{\sqrt{6}}\eta_8 + \frac{1}{\sqrt{3}}\eta_0 & \pi^+ & K^+ \\ \pi^- & -\frac{1}{\sqrt{2}}\pi^0 + \frac{1}{\sqrt{6}}\eta_8 + \frac{1}{\sqrt{3}}\eta_0 & K^0 \\ K^- & \bar{K}^0 & -\frac{2}{\sqrt{6}}\eta_8 + \frac{1}{\sqrt{3}}\eta_0 \end{pmatrix}, \end{aligned} \quad (15)$$

where  $\Phi$  is the field matrix,  $\mathcal{M}$  is the quark mass matrix,  $f_\pi$  is the pion decay constant,  $U$  is the unitary matrix that parametrizes and governs the dynamics of the pseudoscalar fields,  $B_0$  is the constant used to normalize the mass term in such a way that  $M_\pi^2 = B_0(m_u + m_d)$ , and  $m_0$  is the mass term due to the symmetry breaking that gives a significant part of their masses to  $\eta$  and  $\eta'$ . We expand  $U$  in a power series up to second order and retain only the terms that generate particle masses, discarding constant and higher-order terms. Therefore, we obtain:

$$\begin{aligned} -B_0 \langle \mathcal{M} \Phi^2 \rangle &= -B_0(m_u + m_d) \pi^+ \pi^- - B_0(m_u + m_s) K^+ K^- \\ &- B_0(m_d + m_s) K^0 \bar{K}^0 - B_0 \frac{m_u + m_d}{2} \pi^0 \pi^0 \\ &- B_0 \frac{m_u + m_d + 4m_s}{6} \eta_8^2 - B_0 \frac{m_u + m_d + m_s}{3} \eta_0^2 \\ &- B_0 \frac{m_u - m_d}{\sqrt{3}} \pi^0 \eta_8 - B_0 \sqrt{\frac{2}{3}} (m_u - m_d) \pi^0 \eta_0 \\ &- B_0 \frac{\sqrt{2}}{3} (m_u + m_d - 2m_s) \eta_8 \eta_0, \end{aligned} \quad (16)$$

Eq. (16) corresponds to the parametrization  $\mathcal{L}^{\chi\text{PT@LO}} \supset -\frac{1}{2} \phi^T \tilde{M}^2 \phi$  for real scalar fields, where  $\tilde{M}^2$  is the meson mass-squared matrix. Using the isospin limit ( $m_u = m_d$ ) and focusing on the  $\eta_8 - \eta_0$  subspace we attain the following matrix:

$$\tilde{M}_{\eta_8 \eta_0}^2 = \begin{pmatrix} m_{\eta_8}^2 & m_{\eta_8 \eta_0}^2 \\ m_{\eta_8 \eta_0}^2 & m_{\eta_0}^2 \end{pmatrix}, \quad \begin{aligned} m_{\eta_0}^2 &= m_0^2 + \frac{2}{3} B_0 (m_u + m_d + m_s), \\ m_{\eta_8}^2 &= \frac{B_0}{3} (m_u + m_d + 4m_s), \\ m_{\eta_8 \eta_0}^2 &= \frac{\sqrt{2}}{3} B_0 (m_u + m_d - 2m_s). \end{aligned} \quad (17)$$

This matrix can be diagonalized using the rotation shown in Eq. (2). In this case,  $\theta$  can be analytically computed using  $B_0$  and the mass values for quark and  $\eta'$ , acquired from [1]. Thus, we obtain  $\theta = -21.2^\circ$ , which can be related to the mixing angle through Eq. (4), achieving  $\phi = 33.5^\circ$ .

## V. CONCLUSIONS

In this work, we have performed a phenomenological study of the  $D_{(s)}^+ \rightarrow \eta^{(\prime)} \ell^+ \nu_\ell$  and  $B^+ \rightarrow \eta^{(\prime)} \ell^+ \nu_\ell$  decays to extract the  $\eta$ - $\eta'$  mixing angle  $\phi$  in the quark-flavor basis. We have employed two different representations of

the participating form factors, specifically a single pole and dipole (cf. Eqs. (7)).

From fits to most recent differential decay width distributions experimental data we have obtained  $\phi = 40.6(4.8)^\circ$ , while from the analysis of ratios of branching ratios we determined  $\phi = 42.3(3.7)^\circ$ . Interestingly enough our determinations are in very good agreement with a very recent determination from the Lattice QCD Extended Twisted Mass Collaboration,  $\phi = 39.3(2.0)^\circ$ . On the other hand, our values are larger than the naive estimate we calculate from Chiral Perturbation Theory at leading order  $\phi = 33.5^\circ$ . In Fig. 6 we present a summary of our results (red and blue triangles) as compared to the Lattice QCD result (orange square) and the ChPT estimate (green square). We hope our study strengthens the case for new and more precise measurements as it would allow more precise determinations of the  $\eta$ - $\eta'$  mixing.

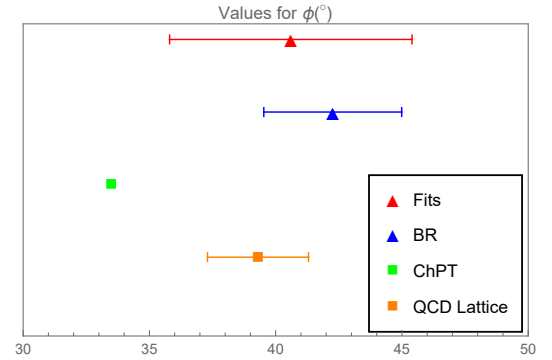


FIG. 6: Summary of our determinations of the  $\eta$ - $\eta'$  mixing angle  $\phi$  and the value obtained from Lattice QCD [6].

## Acknowledgments

This paper has been possible thanks to the unvaluable help and guidance of my advisor Sergi González-Solís. I would also like to thank my family and friends for their support and encouragement, which has been completely necessary for me to arrive this far.

## Bibliography

- [1] S. Navas *et al.* [Particle Data Group], Phys. Rev. D **110** (2024) no.3, 030001
- [2] A. Bazavov *et al.* [Fermilab Lattice and MILC], Phys. Rev. D **107** (2023) no.9, 094516 [arXiv:2212.12648 [hep-lat]].
- [3] M. Ablikim *et al.* [BESIII], [arXiv:2506.02521 [hep-ex]].
- [4] M. Ablikim *et al.* [BESIII], Phys. Rev. Lett. **134** (2025) no.11, 111801 [arXiv:2410.08603 [hep-ex]].
- [5] M. Ablikim *et al.* [BESIII], Phys. Rev. D **108** (2023) no.9,

092003 [arXiv:2306.05194 [hep-ex]].

- [6] K. Ottnad, S. Bacchio, J. Finkenrath, B. Kostrzewa, M. Petschlies, F. Pittler, C. Urbach and U. Wenger, [arXiv:2503.09895 [hep-lat]].
- [7] J. Gasser and H. Leutwyler, Nucl. Phys. B **250** (1985), 465-516



Determinació de la barreja de  $\eta$ - $\eta'$  a partir de les desintegracions dels mesons  $D_{(s)}^+$  i  $B^+$ 

Author: Joel Rastrojo Morote, jrastrmo7@alumnes.ub.edu  
 Facultat de Física, Universitat de Barcelona, Diagonal 645, 08028 Barcelona, Spain.

Advisor: Sergi González-Solís de la Fuente, sergig@fqa.ub.edu

**Resum:** En aquest TFG hem determinat el grau de barreja dels mesons  $\eta$  i  $\eta'$  a partir de les desintegracions semileptòniques  $D_{(s)}^+ \rightarrow \eta^{(\prime)} \ell^+ \nu_\ell$  i  $B^+ \rightarrow \eta^{(\prime)} \ell^+ \nu_\ell$ , emprant dades aportades per la col·laboració BESIII i el PDG. A partir de parametritzar els factors de forma i de mesures experimentals, hem realitzat ajustos a les distribucions diferencials per a les desintegracions, trobant un valor de  $\phi = 40.6(4.8)^\circ$  i realitzant quocients de les proporcions de ramificació hem obtingut un valor de  $\phi = 42.3(3.7)^\circ$ . Aquests valors són compatibles amb els resultats obtinguts recentment a través de Lattice QCD,  $\phi = 39.3(2.0)^\circ$  portat a terme per la col·laboració ETM. Finalment, hem realitzat un càlcul teòric a través de la Teoria de Pertorbacions Quiral, obtenint  $\phi = 33.5^\circ$  el qual és més petit que els obtinguts prèviament al ser una estimació naïf.

**Paraules clau:** Física de l' $\eta$ - $\eta'$ , factors de forma hadrònics, desintegracions semileptòniques

**ODSs:** 4. Educació de qualitat

## Objectius de Desenvolupament Sostenible (ODSs o SDGs)

1. Fi de la es desigualtats	10. Reducció de les desigualtats	
2. Fam zero	11. Ciutats i comunitats sostenibles	
3. Salut i benestar	12. Consum i producció responsables	
4. Educació de qualitat	X 13. Acció climàtica	
5. Igualtat de gènere	14. Vida submarina	
6. Aigua neta i sanejament	15. Vida terrestre	
7. Energia neta i sostenible	16. Pau, justícia i institucions sòlides	
8. Treball digne i creixement econòmic	17. Aliança pels objectius	
9. Indústria, innovació, infraestructures		

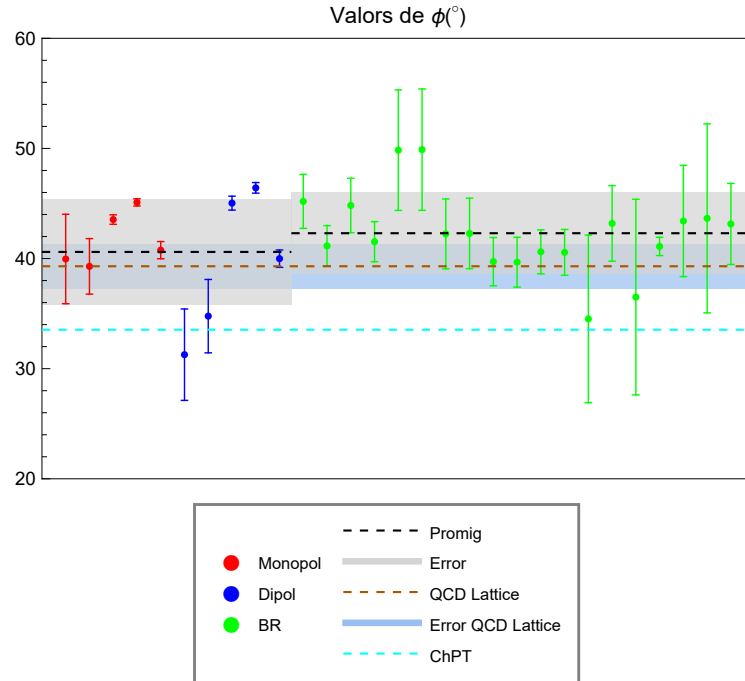


FIG. 7: Gràfica resum dels valors de  $\phi$  obtinguts en aquest treball i comparats amb l'obtingut amb QCD Lattice per la ETM Collaboration.

## Appendix A: SUPPLEMENTARY MATERIAL (OPTIONAL)

TABLE II: Values of the branching ratio for the different decays and it's corresponding dependence of  $\phi$  for their form factor. Data for  $D_s^+ \rightarrow \eta^{(\prime)} \ell^+ \nu_l$ ,  $B^+ \rightarrow \eta^{(\prime)}(\pi^0) \ell^+ \nu_l$  and  $D^+ \rightarrow \pi^0 \ell^+ \nu_l$  are extracted from [1] meanwhile for  $D^+ \rightarrow \eta \ell^+ \nu_l$  and  $D^+ \rightarrow \eta' \ell^+ \nu_l$  are taken from [3] and [4] respectively, which are more precise.

$M_i$	$M_f$	$f(\phi)$	$\ell$	BR(%)
$D^+$	$\eta$	$\cos(\phi)$	$\mu^+$	$9.08(41) \cdot 10^{-2}$
			$e^+$	$9.75(40) \cdot 10^{-2}$
	$\eta'$	$\sin(\phi)$	$\mu^+$	$1.92(29) \cdot 10^{-2}$
			$e^+$	$1.79(20) \cdot 10^{-2}$
	$\pi^0$	1	$\mu^+$	$35.0(1.50) \cdot 10^{-2}$
			$e^+$	$37.2(1.70) \cdot 10^{-2}$
$D_s^+$	$\eta$	$-\sin(\phi)$	$\mu^+$	2.4(0.5)
			$e^+$	2.26(6)
	$\eta'$	$\cos(\phi)$	$\mu^+$	1.1(5)
			$e^+$	$8.0(4) \cdot 10^{-1}$
$B^+$	$\eta$	$\cos(\phi)$	$\ell^+$	$3.5(4) \cdot 10^{-3}$
	$\eta'$	$\sin(\phi)$	$\ell^+$	$2.4(7) \cdot 10^{-3}$
	$\pi^0$	1	$\ell^+$	$7.80(27) \cdot 10^{-3}$

TABLE III: Values and errors for mixing angle calculated through branching ratios quotients for the different decays using data from Table II.

$M_i$	$M_{f_1}$	$M_{f_2}$	$\ell_1$	$\ell_2$	$\phi$ ( $^\circ$ )
$D^+$	$\eta'$	$\eta$	$\mu^+$	$e^+$	45.2(2.4)
		$\eta$	$e^+$	$\mu^+$	41.2(1.8)
		$\eta$	$\mu^+$	$\mu^+$	44.8(2.5)
		$\eta$	$e^+$	$e^+$	41.5(1.8)
		$\pi^0$	$\mu^+$	$\mu^+$	49.8(5.5)
		$\pi^0$	$\mu^+$	$e^+$	49.9(5.5)
		$\pi^0$	$e^+$	$\mu^+$	42.2(3.2)
		$\pi^0$	$e^+$	$e^+$	42.3(3.2)
	$\eta$	$\pi^0$	$\mu^+$	$\mu^+$	39.7(2.2)
		$\pi^0$	$\mu^+$	$e^+$	39.7(2.3)
		$\pi^0$	$e^+$	$\mu^+$	40.6(2.0)
		$\pi^0$	$e^+$	$e^+$	40.6(2.1)
$D_s^+$	$\eta'$	$\eta$	$\mu^+$	$e^+$	34.5(7.6)
		$\eta$	$e^+$	$\mu^+$	43.2(3.4)
		$\eta$	$\mu^+$	$\mu^+$	36.5(8.9)
		$\eta$	$e^+$	$e^+$	41.1(8)
$B^+$	$\eta'$	$\eta$	$\ell^+$	$\ell^+$	43.4(5.0)
		$\pi^0$	$\ell^+$	$\ell^+$	43.7(8.6)
	$\eta$	$\pi^0$	$\ell^+$	$\ell^+$	43.1(3.7)